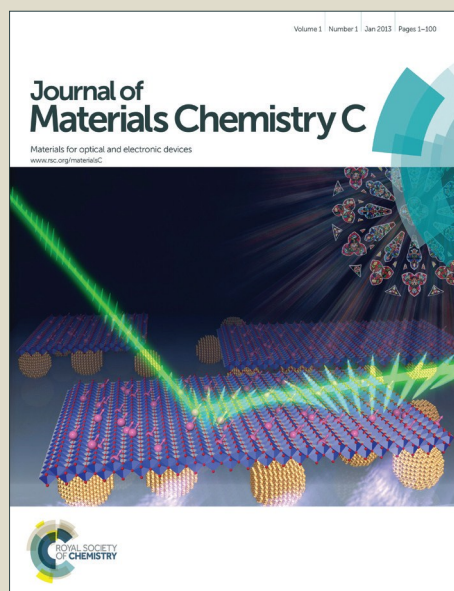


Journal of Materials Chemistry C

Accepted Manuscript



This is an *Accepted Manuscript*, which has been through the Royal Society of Chemistry peer review process and has been accepted for publication.

Accepted Manuscripts are published online shortly after acceptance, before technical editing, formatting and proof reading. Using this free service, authors can make their results available to the community, in citable form, before we publish the edited article. We will replace this *Accepted Manuscript* with the edited and formatted *Advance Article* as soon as it is available.

You can find more information about *Accepted Manuscripts* in the [Information for Authors](#).

Please note that technical editing may introduce minor changes to the text and/or graphics, which may alter content. The journal's standard [Terms & Conditions](#) and the [Ethical guidelines](#) still apply. In no event shall the Royal Society of Chemistry be held responsible for any errors or omissions in this *Accepted Manuscript* or any consequences arising from the use of any information it contains.



ARTICLE

Effect of Alkyl Spacer Length on the Electrical Performance of Diketopyrrolopyrrole-Thiophene Vinylene Thiophene Polymer Semiconductors

Received 00th January 20xx,
Accepted 00th January 20xx

DOI: 10.1039/x0xx00000x

www.rsc.org/

Hojeong Yu,^{a,d} Kwang Hun Park,^b Inho Song,^a Myeong-Jong Kim,^b Yun-Hi Kim^{c,*}, Joon Hak Oh^{a,*}

For systematic investigation of the structure-property relationship, a series of diketopyrrolopyrrole-thiophene vinylene thiophene (DPP-TVT) polymers, ranging from 25-DPP-TVT to 32-DPP-TVT, with branched alkyl groups containing linear spacer groups from C2 to C9, has been synthesized. The electrical performance of these polymers is clearly dependent on the length of the spacer group and shows the odd-even alterations of chemical and electronic properties induced by the different alkyl chain spacers. Spacer groups with even numbers of carbon atoms exhibit higher charge-carrier mobilities than those with odd numbers of carbon atoms for the linear spacer groups from C2 to C7. Furthermore, the optimal side chain geometry in DPP-TVT system for the most efficient charge transport contains C6 spacer between the branching point and the backbone, showing the maximum hole mobility of $8.74 \text{ cm}^2 \text{ V}^{-1} \text{ s}^{-1}$ (at $V_{\text{GS}}, V_{\text{DS}} = -100 \text{ V}$). The results obtained herein demonstrate the intriguing odd-even effects induced by the length of the side chain alkyl spacers for DPP-TVT polymers, and provide insight into the side chain engineering for the most efficient charge transport in DPP-based polymer semiconductors.

Introduction

Optimal molecular design of polymer semiconductors via molecular backbone and side chain engineering has led to remarkable advances in high-performance organic field-effect transistors (OFETs), surpassing the charge carrier mobility of amorphous silicon semiconductors.¹⁻³ State-of-the-art, high-performance polymer semiconductors have been mainly obtained by molecular design for the conjugated backbone unit, mostly adopting alternating electron donor (D) and acceptor (A) building blocks that can enhance intermolecular interactions and intramolecular charge transfer. In recent years, among high-performance polymer backbones, the electron-accepting diketopyrrolopyrrole (DPP) moiety has attracted great interest for constructing high-performance donor-acceptor (D-A) type polymer semiconductors,⁴⁻⁸

showing charge carrier mobilities over $10 \text{ cm}^2 \text{ V}^{-1} \text{ s}^{-1}$.⁹⁻¹³ The rational design of molecular backbones in polymer semiconductors is of great importance, as it intrinsically determines the electronic properties of organic semiconductors.¹⁴⁻¹⁹

Recently, however, it turned out that sophisticated side chain engineering can significantly enhance the charge carrier mobility of *p*-type,²⁰⁻²² *n*-type,^{23, 24} and ambipolar conjugated polymers.²⁵ This is because the length,²⁵⁻²⁷ branching point position,^{12, 20, 28} and bulkiness²⁹ of side chains can also critically affect the physicochemical properties of polymers (i.e., solubility, optical absorption capacity, solid state packing) and consequently influence the molecular packing and π -planar distance closely related to the charge transport.^{1, 30, 31} In particular, the number of carbons in alkyl side chain and/or spacers results in different molecular tilt angles on the deposited substrate. Therefore, depending on the odd or even characteristic of the number of carbon, the extension directions of the side chains in the molecular packing may be determined, and the electrical property of the resulting polymers may be systematically changeable. Such odd-even effects on molecular conformations and packing structures have been widely observed over organic thin films in chemical and/or physical aspects.^{1, 32, 33} Especially, odd-even alterations of chemical and electronic properties of organic thin films have originated from various complex interactions between organic molecules and surfaces (i.e., self-assembled monolayers) or intra/intermolecular interactions.³⁴⁻³⁷ This is because,

^a Department of Chemical Engineering, Pohang University of Science and Technology (POSTECH), Pohang, Gyeongbuk 790-784, South Korea. E-mail: joonhoh@postech.ac.kr

^b School of Materials Science and Engineering and Engineering Research Institute, Gyeongsang National University, Jinju, Gyeongnam 660-701, South Korea

^c Department of Chemistry and Engineering Research Institute, Gyeongsang National University, Jinju, Gyeongnam 660-701, South Korea. E-mail: ykim@gnu.ac.kr

^d School of Energy and Chemical Engineering, Ulsan National Institute of Science and Technology (UNIST), Ulsan 689-798, South Korea.

[†] Electronic Supplementary Information (ESI) available: Synthetic details and characterization data, additional figures (cyclic voltammetry plots, additional XRD analysis data, AFM phase images), FET fabrication and testing. See DOI: 10.1039/x0xx00000x

ARTICLE

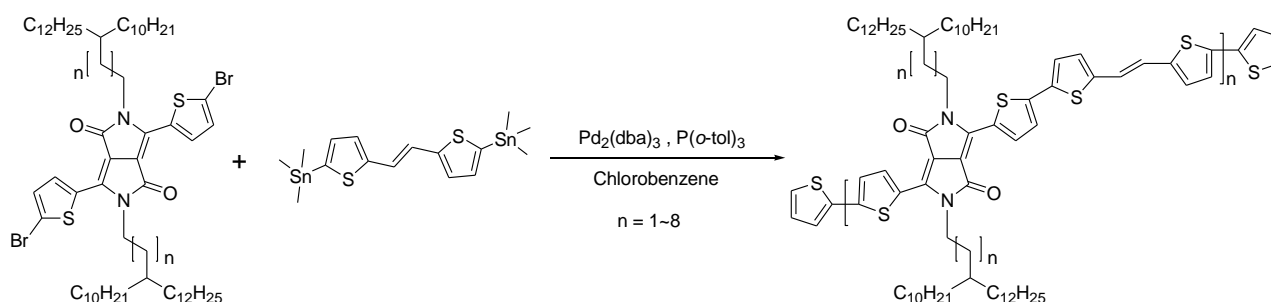
Journal of Materials Chemistry C

depending on the odd or even number of structural units, molecular structural orientations follow the most energetically favorable arrangement. To date, most of odd-even studies have been limited to small molecular organic semiconductors since their packing orientations are simply predicted by theoretical packing analysis.^{1, 32-40} Furthermore, the influence of alkyl chain spacers in the side chains has been mostly investigated using a small number of organic semiconductors containing relatively short alkyl spacers.^{20, 22, 25, 26, 41} Odd-even effects in polymeric system have not been widely investigated so far,³⁸ due to the possibility of free motion of polymer chains.

However, very recently, systematic studies on the effect of side chain branching positions have been reported in polymer semiconductors containing more than six polymers in the series.^{10, 24, 42} In our previous study, we have observed the odd-even effect of the alkyl side chain spacers in the series of diketopyrrolopyrrole-selenophene vinylene selenophene (DPP-SVS) polymers on the molecular packing and morphology, which subsequently affected the charge transport.¹⁰ In this regard, studies on the structure-property relationship of polymer semiconductors with a broad scope of polymer series are highly desirable for the in-depth understanding of the intriguing odd-even effects as well as for providing a molecular design guideline for high-performance polymer semiconductors.

Herein, a new series of poly(diketopyrrolopyrrole-thiophene vinylene thiophene) (PDPP-TVT) polymers with branched alkyl groups containing linear spacer groups (C2 to C9), ranging from 25-DPP-TVT to 32-DPP-TVT, has been synthesized to systematically explore the possibility of odd-even effect on the polymer semiconductor system. The D-A structures in DPP-TVT polymers allow efficient intramolecular charge transfer and facilitate intermolecular interactions. In addition, TVT unit enhances the coplanarity of the conjugated π -backbones for effective molecular packing. The relationship between molecular structure and electrical properties in DPP-based polymer semiconductors has been investigated. The DPP-TVT polymer thin films have been prepared with various solution-based coating methods, such as spin-coating, drop-casting, and solution-shearing techniques. Our results clearly revealed the existence of the odd-even effect on the molecular packing, morphology, and electronic properties in DPP-TVT polymer thin films. Intriguingly, linear alkyl spacer groups with even numbers (C2, C4, C6) showed shorter lattice spacing values than the alkyl spacer groups with odd numbers (C3, C5, C7),

Scheme 1. The synthetic scheme of polymers



leading to higher mobilities and well-connected nanoscale granular domains in thin film morphologies. 31-DPP-TVT and 32-DPP-TVT with the alkyl spacers of C8 and C9 did not show clear odd-even effect, due to increased unpredictable intermolecular interactions between the long alkyl side chains. Among the series of DPP-TVT polymers, 29-DPP-TVT with the alkyl spacer of C6 exhibited the maximum hole mobility of $8.74 \text{ cm}^2 \text{ V}^{-1} \text{ s}^{-1}$, due to the optimized π -planar packing and thin-film morphologies. These findings clearly demonstrate the existence of the odd-even effect of alkyl spacer length on the electrical performance of DPP-based polymer semiconductors, and provide molecular design guidelines for side chains for high-performance polymer semiconductors.

Results and discussion

Synthetic strategies, synthesis, and characterization

A series of DPP-TVT polymers (25-DPP-TVT to 32-DPP-TVT) was synthesized in chlorobenzene solvent for 48 h by a Stille coupling reaction using $\text{Pd}_2(\text{dba})_3$ and $\text{P}(o\text{-Tol})_3$, as shown in Scheme 1. The obtained polymers were purified by precipitation, and successive Soxhlet extraction using methanol, hexane, and chloroform to remove residual monomers and oligomers. The structures of DPP-TVT polymers (25-DPP-TVT to 32-DPP-TVT) were characterized by $^1\text{H-NMR}$ analysis, and elemental analysis of the polymers was also performed (Fig. S1 and Fig. S2 of the ESI[†]). The polymers had good solubility in common organic solvents such as chloroform and chlorobenzene. The average molecular weights of the synthesized polymers were measured by gel permeation chromatography (GPC) using polystyrene standards in *o*-dichlorobenzene. The number average molecular weights (M_n) and polydispersity indexes (PDIs) of polymers are summarized in Table 1. Thermogravimetric analysis (TGA) of 25-DPP-TVT to 32-DPP-TVT revealed their good thermal stability with 5 % weight decomposition up to $335 \sim 428 \text{ }^\circ\text{C}$ (see Fig. S3 and Table S1 of the ESI[†]). In differential scanning calorimetry (DSC) analysis, a distinct phase transition was observed for 25-DPP-TVT and 26-DPP-TVT at $270.9 \text{ }^\circ\text{C}$ and $278.7 \text{ }^\circ\text{C}$, respectively, while no phase transition was observed from 50 to $300 \text{ }^\circ\text{C}$ for 27-DPP-TVT to 32-DPP-TVT (see Fig. S4 and Table S1 of the ESI[†]).

The UV-vis absorption spectra of the DPP-TVT polymer series (25-DPP-TVT to 32-DPP-TVT) in chloroform solution and

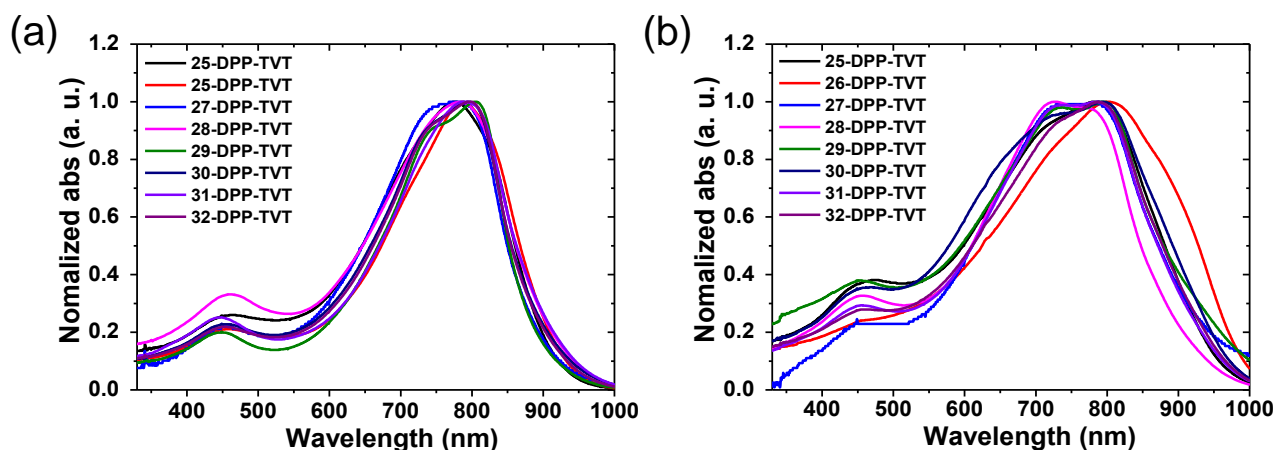


Fig. 1 UV-vis-NIR absorption of the series of DPP-TVT in (a) chloroform solution and (b) thin films.

thin film are displayed in Fig. 1, with the data summarized in Table 1. The polymers exhibit dual optical absorption from 300 to 1000 nm with small high- and intense low-energy bands attributed to the localized π - π^* and internal charge transfer (ICT) transitions, respectively. The absorption maxima of polymer films showed slightly wider and broader absorptions compared with those of solution (Fig. 1). The solution spectra showed slightly red sifted absorption by approximately 10 ~ 12 nm when going from 25-DPP-TVT to 32-DPP-TVT, which may result from the reduced steric hindrance by introducing the larger linear space group between branching point and backbone. Interestingly, the solution and thin film spectra showed distinct dual-bands of 0-1 transition and 0-0 transition, which depended on the odd-even characteristic of the number of linear space groups. This indicates that the close packing of rigid and planar backbone is closely related to the odd-even characteristic of the number of linear space groups. The highest occupied molecular orbital (HOMO) energy levels of all the polymers were measured by cyclic voltammetry, and the resulting HOMO values were between -5.25 eV and -5.28 eV with optical band gaps from 1.23 eV to 1.37 eV (Table 1 and Fig. S5 of the ESI†).

Microstructural analysis of polymer films

The molecular packing and crystallinity of the DPP-TVT polymer series (25-DPP-TVT to 32-DPP-TVT) in film state were investigated by performing out-of-plane X-ray diffraction (XRD) analysis. In the annealed polymer films (200 °C for 10 min), well-defined strong (n00) reflection peaks were observed with higher-order diffraction peaks up to (400) reflections, while the as-cast DPP-TVT films exhibited relatively weak and broad diffraction peaks (Fig. S6 and Table S2 of the ESI†). Interestingly, the series of DPP-TVT polymer films containing the spacer group from C2 to C7 (from 25-DPP-TVT to 30-DPP-TVT) exhibited broadly fluctuating (100) diffraction peaks as shown in Fig. 2a. Such odd-even effect was clearly observed in the average 2θ and d -spacing values of the DPP-TVT polymer films (Fig. 2b) and the corresponding out-of-plane XRD data are summarized in Table 2. These results showed the even-numbered linear spacer groups (25-DPP-TVT with C2, 27-DPP-TVT with C4, 29-DPP-TVT with C6) had shorter d -spacing values than those of the polymers with odd-numbered linear spacer groups (26-DPP-TVT with C3, 28-DPP-TVT with C5, 30-DPP-TVT with C7).

Table 1 Summary of the optical and electrochemical properties, and the number average molecular weight (M_n) and polydispersity of polymers determined by using GPC with polystyrene as the standards.

Polymer	λ_{\max}^{0-0} Sol ^a [nm]	λ_{\max}^{0-1} Sol ^a [nm]	λ_{\max}^{0-0} film ^b [nm]	λ_{\max}^{0-1} film ^b [nm]	Band gap (optical) [eV]	LUMO (optical) [eV]	HOMO (electrochemical) ^c [eV]	M_n^d [kDa] (PDI)
25-DPP-TVT	776	n ^e	785	721	1.31	-3.97	-5.28	633 (1.27)
26-DPP-TVT	784	n	802	n	1.23	-4.03	-5.26	348 (3.28)
27-DPP-TVT	779	742	781	728	1.29	-3.98	-5.27	284 (2.25)
28-DPP-TVT	778	n	778	726	1.37	-3.90	-5.27	49 (5.90)
29-DPP-TVT	799	745	800	734	1.28	-3.97	-5.25	519 (2.67)
30-DPP-TVT	795	n	795	n	1.27	-4.00	-5.27	44 (1.26)
31-DPP-TVT	786	n	787	727	1.32	-3.94	-5.26	179 (3.22)
32-DPP-TVT	791	743	791	736	1.30	-3.97	-5.27	242 (2.39)

^a UV-absorption for solution was measured by using a chloroform solution of 10^{-4} M.

^b UV-absorption for film was measured by spin coating using 0.2 wt% solution.

^c CV was measured in a solution containing Bu_4NClO_4 (0.1 M) in acetonitrile.

^d GPC was measured polystyrene standard in chlorobenzene solvent.

^e Not observed.

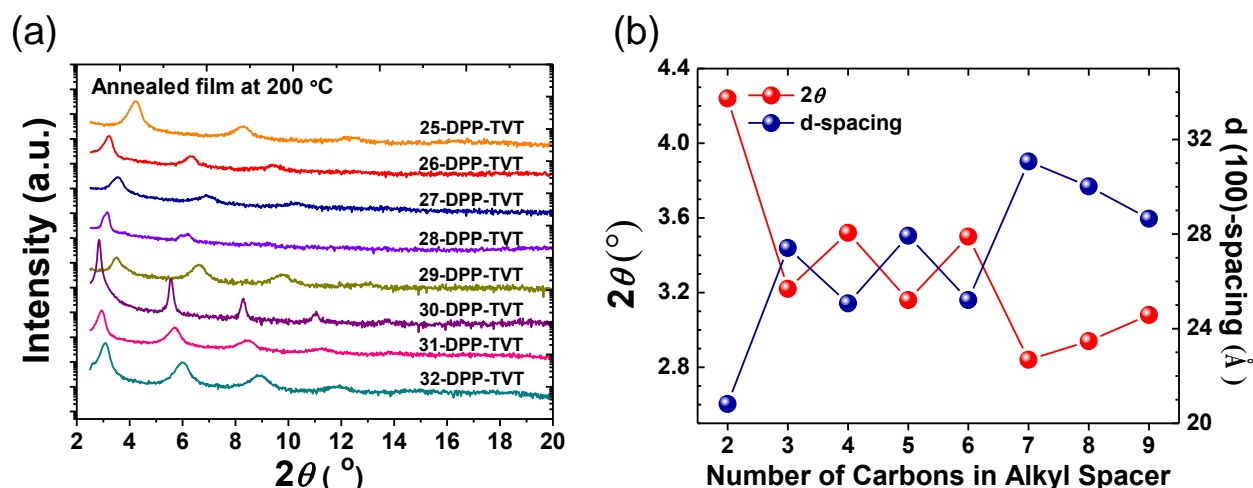


Fig. 2 Out-of-plane XRD diffractogram profile of the series of (a) annealed DPP-TVT films. (b) The average 2θ and $d(100)$ -spacing values of the DPP-TVT polymer films as a function of the number of carbons in side chain.

Table 2 Peak assignments for the out-of-plane XRD intensity profiles obtained from DPP-TVT films under 200 °C thermal annealing.

Polymer	(n00)	2θ (°)	$d(100)$ -spacing (Å)
25-DPP-TVT	(100)	4.24	20.82
	(200)	8.32	-
	(300)	12.38	-
	(400)	16.76	-
26-DPP-TVT	(100)	3.22	27.41
	(200)	6.36	-
	(300)	9.38	-
	(400)	-	-
27-DPP-TVT	(100)	3.52	25.07
	(200)	6.9	-
	(300)	10.26	-
	(400)	13.6	-
28-DPP-TVT	(100)	3.16	27.93
	(200)	6.18	-
	(300)	9.3	-
	(400)	-	-
29-DPP-TVT	(100)	3.5	25.21
	(200)	6.62	-
	(300)	9.84	-
	(400)	13.1	-
30-DPP-TVT	(100)	2.84	31.07
	(200)	5.56	-
	(300)	8.3	-
	(400)	11.06	-
31-DPP-TVT	(100)	2.94	30.02
	(200)	5.7	-
	(300)	8.42	-
	(400)	11.28	-
32-DPP-TVT	(100)	3.08	28.65
	(200)	5.98	-
	(300)	8.9	-
	(400)	11.94	-

This odd-even trend of molecular packing in polymer semiconductors suggests alternation in the molecular packing densities depending on the carbon number of spacer group (not significantly affected by donor group change in DPP-based D-A system). DPP-TVT polymers have linear alkyl chains (C2-C9) as spacers and branched even-numbered n-alkane chains ($C_{12}H_{25}$ and $C_{10}H_{21}$) at the end group position. It is known that the odd/even number of alkyl spacer can determine the extension directions of chains.^{32, 43} Whether the alkyl spacer has an odd/even number of CH_2 groups, a definite odd-even difference in chain conformation or hydrogen bonding between adjacent molecules has been obtained and such principle has been observed from a few of organic small molecules containing $R-(CH_2)_m-R$ ($m=2n$ and $2n+1$) group.³² Our DPP-TVT polymers also clearly showed odd-even difference in d -spacings.

The polymers containing even-numbered linear spacer groups (25-DPP-TVT with C2, 27-DPP-TVT with C4, and 29-DPP-TVT with C6) showed denser molecular packing with smaller d -spacing values than the polymers containing odd-numbered linear spacer groups (26-DPP-TVT with C3, 28-DPP-TVT with C5, and 30-DPP-TVT with C7). However, for the linear alkyl spacers larger than C7, the odd-even effect disappeared due to the unpredictable increased intermolecular interactions of the alkyl side chains. In molecular packing structural analysis of DPP-TVT thin films, it is found that there was no distinguishable difference in odd-even characteristics in between DPP-TVT and DPP-SVS polymer series. The results described herein suggest that odd-even effect is dominantly affected by side chains, not by donor group change in backbone, since the zigzag-like d -spacing variations are mainly originated from the difference in the molecular packing density in the out-of-plane direction.

To further investigate the molecular packing characteristics of DPP-TVT polymer films, the morphologies of the DPP-TVT polymer films annealed at 200 °C were investigated using tapping-mode atomic force microscopy (AFM). Fig. 3 shows the AFM height images ($5\mu m \times 5\mu m$ scan) of polymer films.

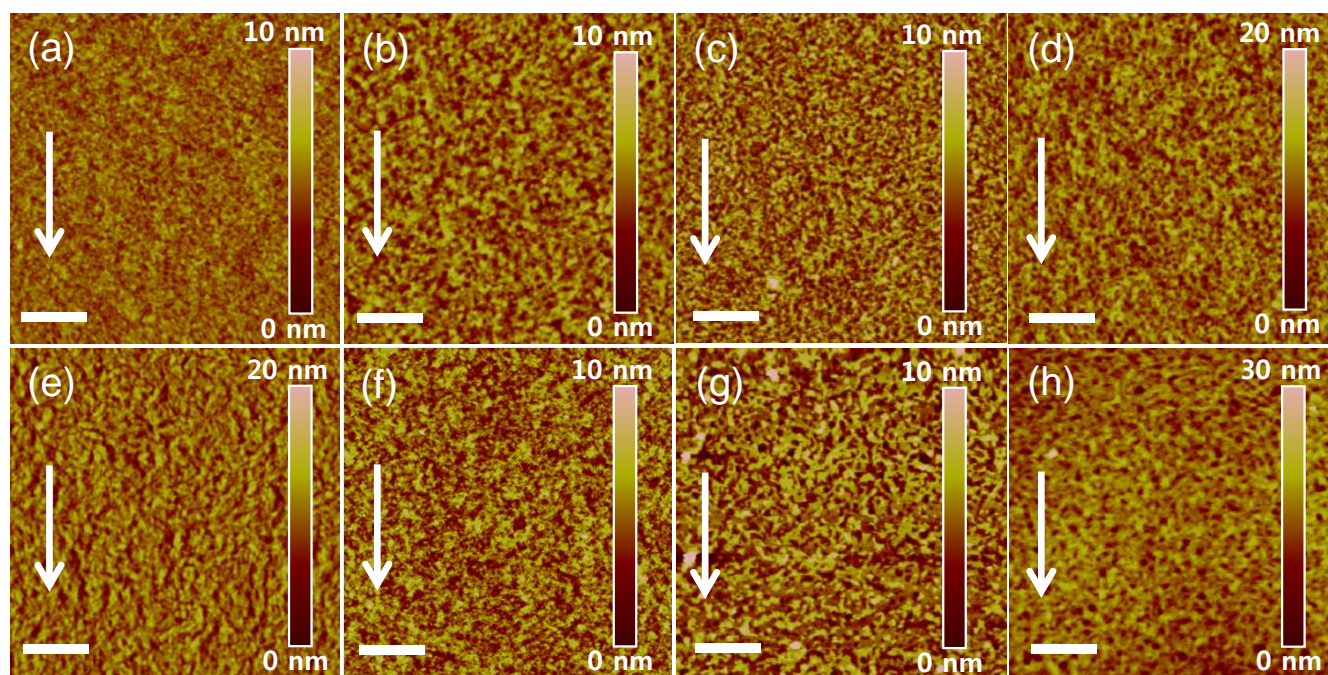


Fig. 3 AFM height image of solution-sheared polymer thin films annealed at 200 °C. Solution-sheared film of (a) 25-DPP-TVT, (b) 26-DPP-TVT, (c) 27-DPP-TVT, (d) 28-DPP-TVT, (e) 29-DPP-TVT, (f) 30-DPP-TVT, (g) 31-DPP-TVT, and (h) 32-DPP-TVT. The shearing direction (top to bottom) is vertical to the scanning direction (left to right). The arrow indicates the direction of shearing. The scale bars represent 1 μm .

The corresponding phase images are presented in Fig. S7 of the ESI[†]. Overall, the polymer films containing even-numbered spacers (25-DPP-TVT with C2, 27-DPP-TVT with C4, 29-DPP-TVT with C6) were composed of nanoscale granular domains with better intergrain connectivity than those in the polymer films containing odd-numbered spacers (26-DPP-TVT with C3, 28-DPP-TVT with C5, 30-DPP-TVT with C7). The root-mean-square (rms) roughness values were 0.73, 1.35, 2.07, and 2.11 nm for the 25-, 27-, 29-, and 31-DPP-TVT polymer films, respectively. In contrast, the polymer films with odd-numbered spacers exhibited ~ 1.2 times higher average rms roughness values (1.17, 2.17, 1.21, and 2.71 nm for the 26-, 28-, 30-, and 32-DPP-TVT polymer films, respectively). Thin films based on 26-DPP-TVT, 28-DPP-TVT, and 30-DPP-TVT molecules showed comparatively unfavorable interconnected grains with larger holes within domain-domain interconnection which can act as charge-trapping sites. Furthermore, compared with the other polymer films, higher rms roughness values with rather unconnected morphology features were observed from 31-DPP-TVT and 32-DPP-TVT polymer films. This might imply that the long alkyl chains partially collapsed over the surface and were more aggregated than the other polymer films. The differences in the inter-domain connectivity and morphology roughness, as well as in the molecular packing structures, were indicative of the existence of the odd-even effect of the alkyl chain spacer in the DPP-TVT thin-film microstructures.

Fabrication of Solution-Processed FETs and I - V Characterizations

To investigate the charge transport property of the series of DPP-TVT polymer films, we fabricated bottom-gate top-contact field-effect transistors (FETs). The polymer solution in

chlorobenzene (0.2 wt%) was coated on *n*-octadecyltrimethoxysilane (OTS)-modified SiO_2/Si substrates using spin coating, drop casting, and solution shearing methods to investigate the changes in the mobility as a function of alkyl chain spacers in FETs. In the solution shearing method,^{25, 44, 45} a small volume of polymer semiconductor solution was placed on OTS-treated Si substrate preheated at a mild temperature of 60 °C. Then, the solution was covered by a shearing substrate and dragged at a controlled speed while keeping the solution between two Si wafers. The experimental details are included in Experimental Section. The electrical performance of FETs based on the solution-processed DPP-TVT polymer films is summarized in Table 3. The DPP-TVT-FETs exhibited typical *p*-channel characteristics and the maximum

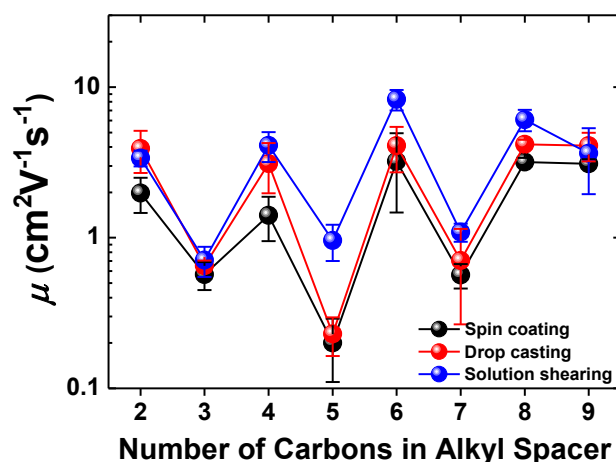


Fig. 4 The average field-effect mobilities obtained from the annealed DPP-TVT thin-film transistors. Distinct odd-even trend with side chain length is observed in a range of 25-DPP-TVT to 32-DPP-TVT.

Table 3 FET performance of DPP-TVT thin films

Conditions ^a		<i>p</i> -channel		
Polymer	Films	$\mu_{h,max}^b$ [cm ² V ⁻¹ s ⁻¹]	$\mu_{h,avg}^c$ [cm ² V ⁻¹ s ⁻¹]	I_{on}/I_{off}
25-DPP-TVT	Spin-coated	2.62	1.98 (±0.27) ^d	>10 ⁴
	Drop-cast	3.59	3.38 (±0.20)	>10 ⁵
	Solution-sheared	4.10	3.91 (±0.61)	>10 ⁶
26-DPP-TVT	Spin-coated	0.63	0.57 (±0.03)	>10 ⁴
	Drop-cast	0.71	0.65 (±0.03)	>10 ⁵
	Solution-sheared	0.80	0.71 (±0.08)	>10 ⁷
27-DPP-TVT	Spin-coated	2.81	1.41 (±0.23)	>10 ³
	Drop-cast	4.35	3.11 (±0.57)	>10 ⁶
	Solution-sheared	4.69	4.10 (±0.46)	>10 ⁶
28-DPP-TVT	Spin-coated	0.23	0.20 (±0.01)	>10 ⁶
	Drop-cast	0.26	0.23 (±0.01)	>10 ⁵
	Solution-sheared	1.20	0.96 (±0.13)	>10 ⁵
29-DPP-TVT	Spin-coated	5.24	3.21 (±0.87)	>10 ⁶
	Drop-cast	5.76	4.08 (±0.68)	>10 ⁷
	Solution-sheared	8.74	8.29 (±0.46)	>10 ⁶
30-DPP-TVT	Spin-coated	0.77	0.57 (±0.14)	>10 ⁵
	Drop-cast	0.90	0.71 (±0.12)	>10 ⁵
	Solution-sheared	1.23	1.09 (±0.08)	>10 ⁵
31-DPP-TVT	Spin-coated	3.60	3.18 (±0.10)	>10 ⁵
	Drop-cast	4.37	4.17 (±0.15)	>10 ⁶
	Solution-sheared	6.69	6.08 (±0.39)	>10 ⁷
32-DPP-TVT	Spin-coated	3.27	3.10 (±0.11)	>10 ⁶
	Drop-cast	4.31	3.64 (±0.66)	>10 ⁶
	Solution-sheared	4.85	4.09 (±0.44)	>10 ⁵

^aThe *p*-channel characteristics of DPP-TVT FETs were measured at $V_{DS} = -100$ V.

^bThe maximum and ^cthe average mobility over 15 FET devices with channel length (*L*) of ~50 μm and channel width (*W*) of ~1000 μm.

^dThe standard deviation.

and the average mobilities were obtained from more than 15 FET devices. Fig. 4 shows the average field-effect mobilities with standard deviation values for the solution-processed FETs based on the DPP-TVT polymer films. Among the various coating methods, the solution-sheared thin films exhibited the highest mobilities due to the aligned and crystalline nature of the solution-sheared films. The corresponding transfer and output characteristics are shown in Fig. S8 of the ESI†. Note that the hole mobilities were calculated in the saturation regime from the transfer curves using a sweep range of ~10 V in the gate voltage due to the rather nonlinear behaviors over the whole sweep range, which might result from several factors, i.e., charge scattering effects induced at a high gate

voltage, contact resistance, gate leakage, or bias stress. Relatively distinct fluctuations in the mobilities were observed within the range of 25-DPP-TVT and 30-DPP-TVT, clearly revealing the odd-even dependence. By utilizing various coating methods with repeated measurements, we could confirm that such enormous odd-even variations in both molecular packing and electrical transport are not simply obtained from experimental fluctuations in error ranges. In addition to the observation of odd-even effect in the hole transport, the optimized side chain-containing molecule was found to be 29-DPP-TVT with C6 spacer unit. The solution-sheared 29-DPP-TVT films showed the highest average hole mobility of 8.29 ± 0.46 cm² V⁻¹ s⁻¹, with the maximum mobility of 8.74 cm² V⁻¹ s⁻¹ at V_{GS} , $V_{DS} = -100$ V, due to their shorter *d*-spacing value and well-interconnected nanoscale granular domains observed by AFM morphology image.

To explore practical applications of the optimized 29-DPP-TVT, photo-responses of 29-DPP-TVT FETs were investigated upon on-and-off switching of polychromatic light ($\lambda = 450 - 650$ nm, $\lambda_{max} = 640$ nm, $P_{max} = 36$ mW cm⁻²) at the transistor off-state ($V_{GS} = 0$ V and $V_{DS} = -100$ V) (Fig. S9 of the ESI†). The photogenerated charge carriers produced noticeable photocurrents in 29-DPP-TVT FETs. Their highly reproducible photosensitivity could substantiate the potential of 29-DPP-TVT for use in photo-sensing applications. In addition, 30-DPP-TVT FETs exhibited much lower performance in contrast to 30-DPP-SVS FETs (the average hole mobility of 30-DPP-TVT was 1.09 ± 0.08 cm² V⁻¹ s⁻¹, while that of 30-DPP-SVS FETs was 9.78 ± 1.64 cm² V⁻¹ s⁻¹ in our previous report¹⁰). This might result from the much larger *d*-spacing value of 30-DPP-TVT thin film than that of 30-DPP-SVS, leading to unfavorable charge transport in OFET performance (the *d*-spacing of 30-DPP-TVT was 31.07 Å, while the *d*-spacing of 30-DPP-SVS was 28.0 Å). On the other hand, slight variations in the mobility were observed by increasing the side chain length (number) above 30-DPP-TVT. Such variation in the odd-even effect was consistent with the results from XRD and AFM analyses.

Experimental

AFM characterization

An Agilent 5500 (Agilent, USA) scanning probe microscope (SPM) equipped with a Nanoscope V controller was used to obtain AFM images of DPP-TVT thin films. AFM images were recorded in high-resolution tapping mode under ambient conditions.

FET fabrication and testing

FET devices with bottom-gate top-contact configuration were prepared to characterize the electrical performance of the series of DPP-TVT. A highly *n*-doped (100) Si wafer (< 0.004 Ω·cm) with a thermally grown SiO₂ (300 nm, $C_i = 10$ nF cm⁻²) was utilized as the substrate and dielectric. The surface of SiO₂ was modified with *n*-octadecyltrimethoxysilane (OTS) self-assembled monolayer (SAM) as previously reported.^{37, 46, 47} 3 mM of OTS solution in trichloroethylene was spin-coated on the piranha-cleaned wafer at 3000 rpm for 30 s. Then, the wafer was exposed to ammonia vapor for ~12 h to facilitate the formation of OTS SAM, followed by sonication cleaning,

sequential washing, and drying. The contact angle on the hydrophobic OTS-modified wafer with D.I. water droplet was $> 106^\circ$. The DPP-TVT polymers were dissolved in chlorobenzene (0.2 wt%) and the film was prepared on the substrate by various solution-processing methods; spin-coating, drop-casting, and solution-shearing.^{44, 45} In solution-shearing, substrate temperature and shearing speed were optimized to 60°C and 0.12 mm s^{-1} , respectively for thin film formation (thickness $< 30\text{ nm}$). Then, the polymer thin-film was annealed on a hot plate at 200°C for 10 min under N_2 atmosphere. Gold contacts (40 nm) were thermally evaporated onto the polymer film to form source and drain electrodes with a channel length (L) of $\sim 50\text{ }\mu\text{m}$ and a channel width (W) of $\sim 1000\text{ }\mu\text{m}$ using shadow mask. The electrical performance of FETs was measured in a N_2 -filled glove box using a Keithley 4200 semiconductor parametric analyzer. The field-effect mobility was calculated in the saturation regime using the following equation:

$$I_D = \frac{W}{2L} \mu C_i (V_{GS} - V_T)^2$$

where I_D is the drain-to-source current, W and L are the semiconductor channel width and length, respectively, μ is the mobility, and V_{GS} and V_T are the gate voltage and threshold voltage, respectively.

Conclusion

A series of DPP-TVT polymers ranging from 25-DPP-TVT to 32-DPP-TVT, with branched alkyl groups containing linear spacer groups from C2 to C9, was synthesized to systematically investigate the structure-property relationship, especially to study on the odd-even effect induced by the number of carbon atoms in the alkyl spacer of the DPP-TVT polymer side chains. The solid-state molecular packing density and charge transport capability were clearly altered, depending on whether the number was odd or even. Linear alkyl spacer groups with even numbers of carbon atoms (C2, C4, C6) exhibited shorter lattice spacings than did spacer groups with odd numbers of carbon atoms (C3, C5, C7), resulting in higher hole mobilities. The optimal alkyl spacer length was confirmed by the series of DPP-TVT polymers and 29-DPP-TVT containing C6 linear spacer group exhibited the maximum hole mobility of $8.74\text{ cm}^2\text{V}^{-1}\text{s}^{-1}$ (V_{GS} , $V_{DS} = -100\text{ V}$). Our findings systematically confirm the existence of odd-even effects as a function of alkyl spacer length in the side chain of DPP-based polymer semiconductors. The optimized side chain geometry with the alkyl spacer of C6 effectively facilitated charge transport via the synergistic effect of optimized molecular packing and film morphology. Our results provide practical guidelines for the side chain engineering to develop high-performance polymer semiconductors.

Acknowledgements

This work was supported by the Center for Advanced Soft Electronics under the Global Frontier Research Program (2013M3A6A5073175 and 2013M3A6A5073172) of the Ministry of Science, ICT and Future Planning, and by the National Research Foundation of Korea (2014R1A2A2A01007467 and 2012R1A2A2A06047047). H.Y. acknowledges financial support from the Global Ph.D. Fellowship.

References

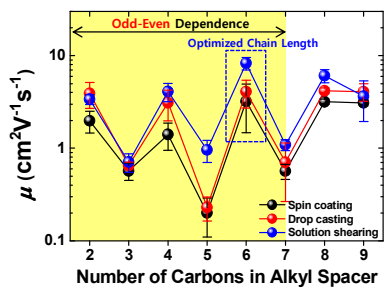
1. J. Mei, Y. Diao, A. L. Appleton, L. Fang and Z. Bao, *J. Am. Chem. Soc.*, 2013, **135**, 6724-6746.
2. H. Sirringhaus, *Adv. Mater.*, 2014, **26**, 1319-1335.
3. H. Dong, X. Fu, J. Liu, Z. Wang and W. Hu, *Adv. Mater.*, 2013, **25**, 6158-6183.
4. T. L. Nelson, T. M. Young, J. Y. Liu, S. P. Mishra, J. A. Belot, C. L. Balliet, A. E. Javier, T. Kowalewski and R. D. McCullough, *Adv. Mater.*, 2010, **22**, 4617-4621.
5. S. C. Ng, H. S. O. Chan, T. T. Ong, K. Kumura, Y. Mazaki and K. Kobayashi, *Macromolecules*, 1998, **31**, 1221-1228.
6. Y. Zhao, Y. Guo and Y. Liu, *Adv. Mater.*, 2013, **25**, 5372-5391.
7. W. Y. Lee, G. Giri, Y. Diao, C. J. Tassone, J. R. Matthews, M. L. Sorensen, S. C. B. Mannsfeld, W. C. Chen, H. H. Fong, J. B. H. Tok, M. F. Toney, M. Q. He and Z. Bao, *Adv. Funct. Mater.*, 2014, **24**, 3524-3534.
8. H.-J. Yun, H. H. Choi, S.-K. Kwon, Y.-H. Kim and K. Cho, *Chem. Mater.*, 2014, **26**, 3928-3937.
9. H.-R. Tseng, H. Phan, C. Luo, M. Wang, L. A. Perez, S. N. Patel, L. Ying, E. J. Kramer, T.-Q. Nguyen, G. C. Bazan and A. J. Heeger, *Adv. Mater.*, 2014, **26**, 2993-2998.
10. J. Y. Back, H. Yu, I. Song, I. Kang, H. Ahn, T. J. Shin, S.-K. Kwon, J. H. Oh and Y.-H. Kim, *Chem. Mater.*, 2015, **27**, 1732-1739.
11. J. Li, Y. Zhao, H. S. Tan, Y. Guo, C. A. Di, G. Yu, Y. Liu, M. Lin, S. H. Lim, Y. Zhou, H. Su and B. S. Ong, *Sci. Rep.*, 2012, **2**, 754.
12. I. Kang, H. J. Yun, D. S. Chung, S. K. Kwon and Y. H. Kim, *J. Am. Chem. Soc.*, 2013, **135**, 14896-14899.
13. A. R. Han, G. K. Dutta, J. Lee, H. R. Lee, S. M. Lee, H. Ahn, T. J. Shin, J. H. Oh and C. Yang, *Adv. Funct. Mater.*, 2015, **25**, 247-254.
14. K. Takimiya, I. Osaka and M. Nakano, *Chem. Mater.*, 2014, **26**, 587-593.
15. W. Jiang, Y. Li and Z. H. Wang, *Chem. Soc. Rev.*, 2013, **42**, 6113-6127.
16. W. P. Wu, Y. Q. Liu and D. B. Zhu, *Chem. Soc. Rev.*, 2010, **39**, 1489-1502.
17. Z. Chen, M. J. Lee, R. Shahid Ashraf, Y. Gu, S. Albert-Seifried, M. Meedom Nielsen, B. Schroeder, T. D. Anthopoulos, M. Heeney, I. McCulloch and H. Sirringhaus, *Adv. Mater.*, 2012, **24**, 647-652.
18. J. D. Yuen, J. Fan, J. Seifter, B. Lim, R. Hufschmid, A. J. Heeger and F. Wudl, *J. Am. Chem. Soc.*, 2011, **133**, 20799-20807.
19. T. Lei, Y. Cao, Y. L. Fan, C. J. Liu, S. C. Yuan and J. Pei, *J. Am. Chem. Soc.*, 2011, **133**, 6099-6101.
20. T. Lei, J. H. Dou and J. Pei, *Adv. Mater.*, 2012, **24**, 6457-6461.

ARTICLE

Journal of Materials Chemistry C

21. B. Fu, J. Baltazar, A. R. Sankar, P.-H. Chu, S. Zhang, D. M. Collard and E. Reichmanis, *Adv. Funct. Mater.*, 2014, **24**, 3734-3744.
22. I. Meager, R. S. Ashraf, S. Mollinger, B. C. Schroeder, H. Bronstein, D. Beatrup, M. S. Vezie, T. Kirchartz, A. Salleo, J. Nelson and I. McCulloch, *J. Am. Chem. Soc.*, 2013, **135**, 11537-11540.
23. F. J. Zhang, Y. B. Hu, T. Schuettfort, C. A. Di, X. K. Gao, C. R. McNeill, L. Thomsen, S. C. B. Mannsfeld, W. Yuan, H. Sirringhaus and D. B. Zhu, *J. Am. Chem. Soc.*, 2013, **135**, 2338-2349.
24. J.-H. Dou, Y.-Q. Zheng, T. Lei, S.-D. Zhang, Z. Wang, W.-B. Zhang, J.-Y. Wang and J. Pei, *Adv. Funct. Mater.*, 2014, **24**, 6270-6278.
25. J. Lee, A. R. Han, H. Yu, T. J. Shin, C. Yang and J. H. Oh, *J. Am. Chem. Soc.*, 2013, **135**, 9540-9547.
26. J. Lee, A. R. Han, J. Kim, Y. Kim, J. H. Oh and C. Yang, *J. Am. Chem. Soc.*, 2012, **134**, 20713-20721.
27. H. J. Chen, Y. L. Guo, G. Yu, Y. Zhao, J. Zhang, D. Gao, H. T. Liu and Y. Q. Liu, *Adv. Mater.*, 2012, **24**, 4618-4622.
28. J. Mei, D. H. Kim, A. L. Ayzner, M. F. Toney and Z. Bao, *J. Am. Chem. Soc.*, 2011, **133**, 20130-20133.
29. K. R. Graham, C. Cabanetos, J. P. Jahnke, M. N. Idso, A. El Labban, G. O. Ngongang Ndjawa, T. Heumueller, K. Vandewal, A. Salleo, B. F. Chmelka, A. Amassian, P. M. Beaujuge and M. D. McGehee, *J. Am. Chem. Soc.*, 2014, **136**, 9608-9618.
30. T. Lei, J. Y. Wang and J. Pei, *Chem. Mater.*, 2014, **26**, 594-603.
31. J. Mei and Z. Bao, *Chem. Mater.*, 2014, **26**, 604-615.
32. F. Tao and S. L. Bernasek, *Chem. Rev.*, 2007, **107**, 1408-1453.
33. H. B. Akkerman, S. C. B. Mannsfeld, A. P. Kaushik, E. Verploegen, L. Burnier, A. P. Zoombelt, J. D. Saathoff, S. Hong, S. Atahan-Evrenk, X. L. Liu, A. Aspuru-Guzik, M. F. Toney, P. Clancy and Z. Bao, *J. Am. Chem. Soc.*, 2013, **135**, 11006-11014.
34. J. H. Oh, W. Y. Lee, T. Noe, W. C. Chen, M. Konemann and Z. Bao, *J. Am. Chem. Soc.*, 2011, **133**, 4204-4207.
35. K. H. Kim, H. Yu, H. Kang, D. J. Kang, C. H. Cho, H. H. Cho, J. H. Oh and B. J. Kim, *J. Mater. Chem. A*, 2013, **1**, 14538-14547.
36. M. Gsanger, J. H. Oh, M. Konemann, H. W. Hoffken, A. M. Krause, Z. Bao and F. Wurthner, *Angew. Chem. Int. Ed.*, 2010, **49**, 740-743.
37. R. Schmidt, J. H. Oh, Y. S. Sun, M. Deppisch, A. M. Krause, K. Radacki, H. Braunschweig, M. Konemann, P. Erk, Z. Bao and F. Wurthner, *J. Am. Chem. Soc.*, 2009, **131**, 6215-6228.
38. R. Marty, R. Nigon, D. Leite and H. Frauenrath, *J. Am. Chem. Soc.*, 2014, **136**, 3919-3927.
39. H. Ebata, T. Izawa, E. Miyazaki, K. Takimiya, M. Ikeda, H. Kuwabara and T. Yui, *J. Am. Chem. Soc.*, 2007, **129**, 15732-15733.
40. X.-Y. Wang, F.-D. Zhuang, X. Zhou, D.-C. Yang, J.-Y. Wang and J. Pei, *J. Mater. Chem. C*, 2014, **2**, 8152-8161.
41. S. Chen, B. Sun, W. Hong, H. Aziz, Y. Meng and Y. Li, *J. Mater. Chem. C*, 2014, **2**, 2183-2190.
42. J. Mei, H.-C. Wu, Y. Diao, A. Appleton, H. Wang, Y. Zhou, W.-Y. Lee, T. Kurosawa, W.-C. Chen and Z. Bao, *Adv. Funct. Mater.*, 2015, **25**, 3455-3462.
43. T. Toledano, H. Sazan, S. Mukhopadhyay, H. Alon, K. Lerman, T. Bendikov, D. T. Major, C. N. Sukenik, A. Vilan and D. Cahen, *Langmuir*, 2014, **30**, 13596-13605.
44. G. Giri, E. Verploegen, S. C. Mannsfeld, S. Atahan-Evrenk, H. Kim do, S. Y. Lee, H. A. Becerril, A. Aspuru-Guzik, M. F. Toney and Z. Bao, *Nature*, 2011, **480**, 504-508.
45. H. A. Becerril, M. E. Roberts, Z. H. Liu, J. Locklin and Z. Bao, *Adv. Mater.*, 2008, **20**, 2588-2594.
46. Y. Ito, A. A. Virkar, S. Mannsfeld, J. H. Oh, M. Toney, J. Locklin and Z. Bao, *J. Am. Chem. Soc.*, 2009, **131**, 9396-9404.
47. A. Virkar, S. Mannsfeld, J. H. Oh, M. F. Toney, Y. H. Tan, G. Y. Liu, J. C. Scott, R. Miller and Z. Bao, *Adv. Funct. Mater.*, 2009, **19**, 1962-1970.

A table of contents entry



Systematic side-chain engineering through adjustment of spacer groups in diketopyrrolopyrrole-thiophene vinylene thiophene (DPP-TVT) polymers reveals odd-even dependence of device performance.